Supporting Information for "Targeting a Rate Promoting Vibration with an Allosteric Mediator in Lactate Dehydrogenase"

Michael W. Dzierlenga and Steven D. Schwartz*

Department of Chemistry and Biochemistry, University of Arizona

E-mail: sschwartz@email.arizona.edu

Computational Methods

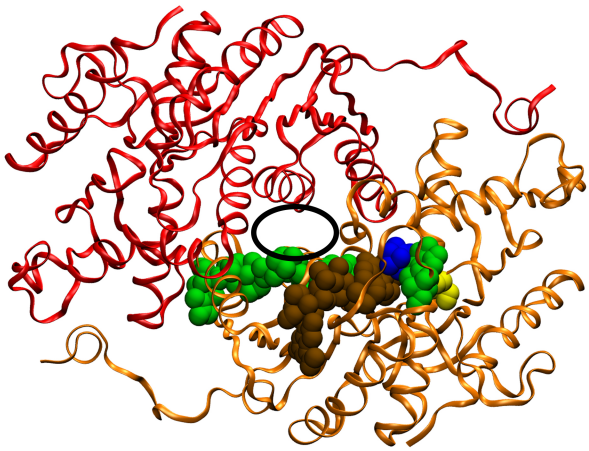

Figure S1: Structure of LDH with two of four monomers (red and orange) and the binding site (black ellipse) shown. The RPV (green), reactive NAD (brown), reactive pyruvate (blue), and reactive histidine (yellow) are highlighted.

The study began with the crystal structure for human heart LDH (PDB accession number 1I0Z)[1]. After choosing the site near the rate promoting vibration and active site shown Figure S1, we examined the residues around the site to design complementary molecules. Once designed, LigPrep[2] was used to prepare the molecules for docking which followed. Docking was performed on the crystal structure and used Glide standard precision docking.[3–6] In total 158 different molecules were docked to this site, and the names and docking scores of these molecules can be found in Table 1 at the end of the supporting information. Binding interactions of the molecule with the best docking score, 2-chloro-N-(3,5-dihydroxyphenyl)acetamide (CPA), can be seen in Figure S2, which was generated using Maestro.

To prepare the system for molecular dynamics, the substrate in the crystal structure, oxamate, was changed to pyruvate by changing the amine group to a methyl group. Hydrogen atoms were added to the crystal structure using the built-in HBUILD command from the CHARMM program[7,8]. The system was then partitioned into quantum molecular (QM) and molecular mechanical (MM) regions. The QM region included the pyruvate, His193, which was protonated to prepare the system for reaction, and the nicotinamide ring of NADH. The C1 of the ribose ring of NADH and

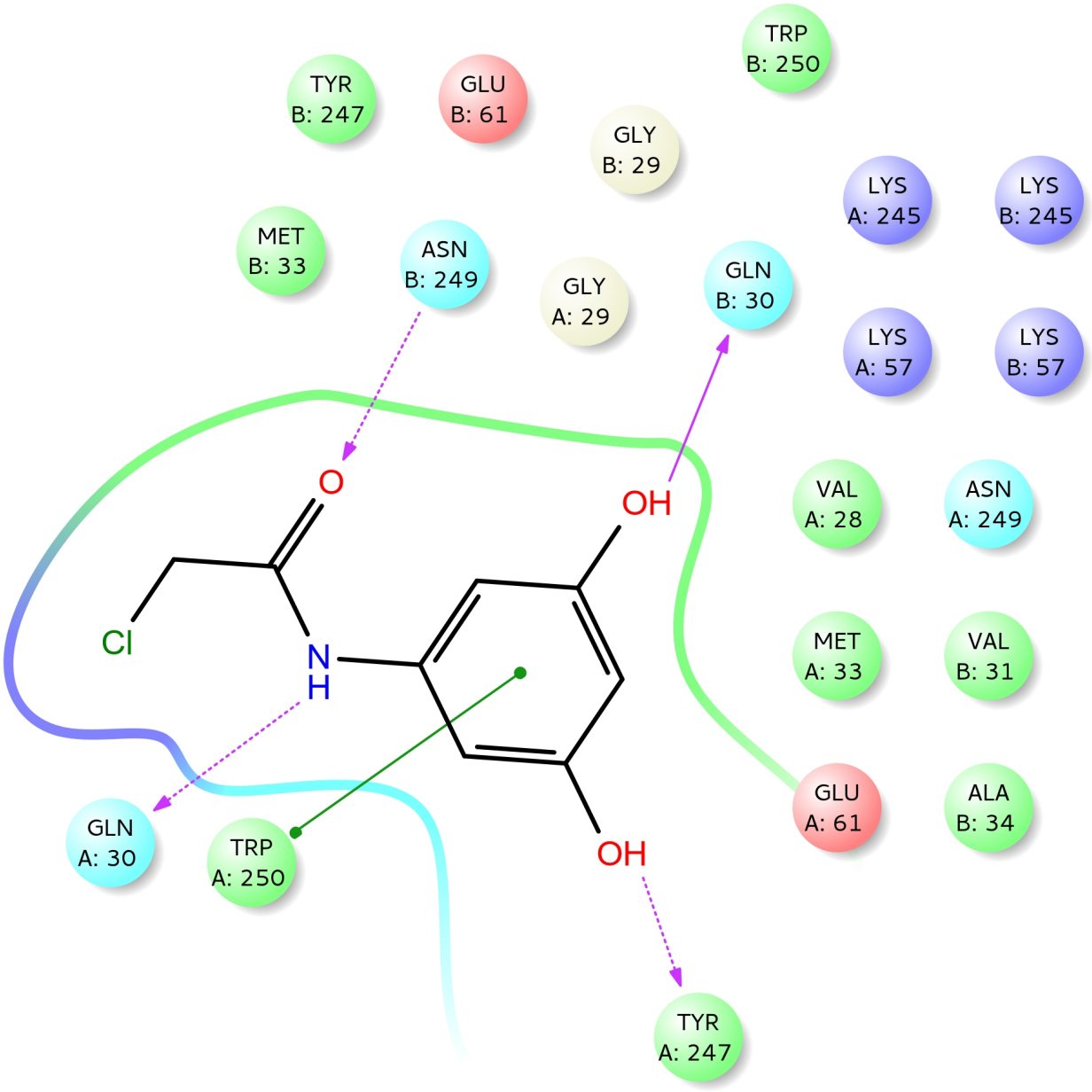

Figure S2: Interactions between CPA and the binding pocket within a 4 Å cutoff from the molecule. The binding pocket is at the interface between the A and B protein monomers.

the α-carbon of His193 were the boundary atoms for the QM and MM regions and were modeled by the generalized hybrid orbital (GHO) method[9]. The quantum mechanical region was modeled using the AM1 method[10], and the rest of the system was modeled using the CHARMM27 force-field[11]. This QM/MM scheme is similar to how our group has studied this system in previous

studies[12–15]. The oxamate in the non-reactive active sites were also changed to pyruvate, but were modeled classically with parameters generated using the CHARMM general force-field.[16–18] The system was solvated in a 60 Å sphere of TIP3P water,[19] in addition to the crystallographic waters already present in the system, and neutralized with 35 potassium ions. At this point the system was duplicated for the preparation of two different ensembles, one without a bound molecule and one with CPA.

For the CPA system, CPA was added to the docking site with overlapping water molecules deleted. Both systems were minimized with 50 steps of steepest-descent, followed by 1200 steps of adopted basis Newton-Raphson minimization with constraints on the non-water atoms that were reduced as the minimization continued. Both systems were heated to 300 K over 300 ps of molecular dynamics. For molecular dynamics a standard time step of 1 fs was used. The systems were then equilibrated for an additional 300 ps. A 0.5 ns production run followed the equilibration to observe the short-timescale non-reactive dynamics with and without CPA.

For TPS, a single microcanonical ensemble was generated for each of the systems. To generate the initial reactive trajectory, harmonic constraints were applied to the donor and acceptor of both the hydride and proton and to the hydride-acceptor and proton-acceptor distances. This was done several times with decreasing constraints to achieve trajectories with minimal biasing potentials. For both the control and the CPA ensembles, 200 trajectories were generated, with acceptance ratios of 31.0% and 29.5% respectively. Committors were calculated for every 20 trajectories in each ensemble. Committor distribution analysis was undertaken with three different sets of constraints. The first constrained only the quantum region of the system. This should constrain almost all the crucial motions for the reaction, including donor-acceptor compressions, donor-particle and acceptor-particle motions, and all histidine and nicotinamide ring motion, but it does not constrain any protein motions that might play a role in the reaction. The second set of constraints is on the quantum region and on the residues identified as part of the rate promoting vibration. The protein was constrained using harmonic distance constraints, R106 β-carbon to the hydride acceptor, V31 β-carbon to the hydride donor, G32 α-carbon to V31 β-carbon, and M33 β-carbon to G32

α-carbon. The third set of constraints were the alternative RPV constraints and were different only in that R106 was constrained to the hydride acceptor by the ζ-carbon instead of the β-carbon. For the distance constraints, the equilibrium value was the value at the transition-state value and the force constant for all constraints was 1,000 kcal/(mol Å^2).

Docking Scores

Table 1: Glide docking scores for the molecules which were docked to the binding site in LDH, sorted by increasing docking score. Docking calculations with score "Failed" were unsuccessful in finding a binding configuration.

Molecules	Glide Score
2-chloro-N-(3,5-dihydroxyphenyl)acetamide	-7.167
2-bromo-N-(3,5-dihydroxyphenyl)acetamide	-7.159
3,5-dihydroxybenzamide	-6.941
2-hydroxy-N-(3,5-hydroxyphenyl)acetamide	-6.934
1-(3,5-hydroxyphenyl)-1H-pyrrole-3-chloro-2,5-dione	-6.921
3-acetamidophenol	-6.859
1-(3,5-hydroxyphenyl)-1H-pyrrole-2,5-dione	-6.760
1-(3,5-hydroxyphenyl)-1H-pyrrole-3-hydroxy-2,5-dione	-6.748
2-bromo-N-(3-hydroxyphenyl)acetamide	-6.722
2-chloro-N-(2,3,5-trihydroxyphenyl)acetamide	-6.646
(2-furyl)oxoacetamide	-6.607
2-acetamidothiophene	-6.480
N-(3,5-dihydroxyphenyl)formamide	-6.457
2-chloro-2-hydroxy-N-(3,5-dihydroxyphenyl)acetamide	-6.413
N-(3-furyl)acetamide	-6.394
2-chloro-N-(3-hydroxyphenyl)acetamide	-6.343
2-hydroxy-N-(3-hydroxyphenyl)acetamide	-6.314

2-(2-chloroacetamido)-thiophene	-6.286
1-(3,5-hydroxyphenyl)-1H-pyrrole-3-methyl-2,5-dione	-6.220
acetanilide	-6.165
5-ethyl-1,3-benzenediol	-6.120
phenylacetamide	-6.089
2-chloro-N-(3,5-dihydroxyphenyl)propanamide	-6.084
gly-tyr dipeptide	-6.055
2-(2-furyl)acetamide	-5.957
N-(3-methoxyphenyl)acetamide	-5.908
L-5-hydroxy-tryptophan	-5.868
orcinol	-5.819
paracetemol	-5.740
N-(2-furanyl)-2-(2-furanyl)-acetamide	-5.735
2-chloro-2-hydroxy-N-(3,5-dihydroxyphenyl)acetamide	-5.727
2-chloro-N-(3-ethoxyphenyl)acetamide	-5.622
1-(3,5-chlorophenyl)-1H-pyrrole-3-chloro-2,5-dione	-5.596
N-benzylacetamide	-5.579
1-(3,5-hydroxyphenyl)-1H-pyrrole-3,4-dichloro-2,5-dione	-5.538
3-phenylpropanamide	-5.537
5,6-dihydroxy-2-benzofuran-1(3H)-one	-5.506
propylsulfonamide	-5.501
isobutylsulfonamide	-5.449
chlorzoxazone	-5.403
N-furanylacetamide	-5.378
L-tryptophan	-5.342
sinapylalcohol	-5.308

2-carboxy-4-acetamido-thiophene	-5.305
2-(2-chloroacetamido)-3,4-hydroxythiophene	-5.285
1,3,2-benzodioxaphosphol-2-ol-2-oxide	-5.226
N-(3-choloro-2-furanyl)-2-(3-choloro-2-furanyl)-acetamide	-5.224
furo[3,4-b]pyrazine-2,3(1H,4H)-dione	-5.207
2-hydroxyl-isobutylsulfonamide	-5.109
acetovanillone	-5.108
di(1,2-hydroxyethyl)sulfoxide	-5.093
2-chloro-N-(3-methoxyphenyl)acetamide	-5.080
6-indolinecarboxylic acid	-5.069
phenyl(diethyl)phosphine	-5.060
2-(2-chloroacetamido)-3,4-hydroxythiophene	-5.047
isovanillin	-5.027
isopropylsulfonamide	-4.946
4-phenylbutanamide	-4.943
trishydroxymethylisobutylsulfoxide	-4.940
vanillin	-4.939
isatin	-4.925
phenyl(ethyl)(carbamoyl)phosphine	-4.906
1H-indole-6-carboxylic acid	-4.845
D-tryptophan	-4.844
5-hydroxyethyl-1,3-benzenediol	-4.816
4-methylhydroxy-5-hydroxyinden-1one	-4.786
2,2,2-trichloro-N-(3,5-dihydroxyphenyl)acetamide	-4.769
4-isopropyl-2-furanamine -1	-4.767
3-(2-chloroacetamido)-5-hydroxythiophene	-4.762

actarit	-4.758
diethylsulfoxide	-4.755
benzylacetamide	-4.738
2-chloro-3-acetamidobenzofuran	-4.737
2-hydroxyl-1-(4-hydroxy-3-methoxyphenyl)ethanone	-4.732
2-chloro-N-(3,5-dihydroxyphenyl)propanamide	-4.695
2-furan-2-amine-3-hydroxylbutyricacid	-4.685
3-(1H-Indol-3-yl)propanamide	-4.682
5-(2-furyl)-5-methyl-2,4-imidazolidinedione	-4.679
piperonal	-4.675
4-chloro-3,5-dihydroxybenzoic acid	-4.577
trishydroxymethylbutysulfoxide	-4.574
ethylsulfonamide	-4.572
digallic acid	-4.525
2-(2-chloroacetamido)-3,4-hydroxythiophene	-4.520
gly-phe dipeptide	-4.510
5-(2-furyl)-5-methyl-2,4-imidazolidinedione	-4.487
phenyl(dimethyl)phosphine	-4.465
3-hydroxylpropanoicacid-2-furanamine -2	-4.428
2-chloro-N-(3,4,5-trihydroxyphenyl)acetamide	-4.423
N-propyl-gallate	-4.421
methyl-acetovanillone	-4.413
2-hydroxy-N-(3,5-dihydroxyphenyl)propanamide	-4.412
oxindole	-4.394
2-chloro-N-(2,3,5,6-tetrahydroxyphenyl)acetamide	-4.392
safrole	-4.386

N-(3-hydroxyphenyl)propanamide	-4.357
eudesmic acid	-4.320
2-hydroxy-N-(3,5-dihydroxyphenyl)propanamide	-4.315
tetrahydroxy-1,4-benzoquinone	-4.293
gallic acid	-4.218
2-furan-2-amine-2-hydroxylbutyricacid	-4.147
dihydroxyethylsulfoxide	-4.127
chlorpropham	-4.115
hydroxymethylpropylsulfoxide	-4.093
diethylether	-4.090
4-hydroxy-5-methylhydroxyinden-1-one	-4.085
gly-phe dipeptide	-4.071
inden-1-one	-4.064
2-furanamine-3-butyricacid	-4.046
gallic acid amide	-4.007
2-chloro-N-(2,5-dimethoxyphenyl)acetamide	-3.990
N-(4-choloro-2-furanyl)-2-(4-choloro-2-furanyl)-acetamide	-3.942
3-hydroxylpropanoicacid-2-furanamine -1	-3.894
2,5-bis(dimethylamino)-1,4-benzoquinone	-3.888
2-(3-chlorophenoxy)-N-(2,3-dihydro-1,4-benzodioxin-6-yl)acetamide	-3.859
p-tolylphosphonate	-3.841
dipropylsulfoxide	-3.772
2-furanamine-3-phenolylpropanoicacid	-3.751
3,5-dimethoxybenzamide	-3.726
p-coumaricacid	-3.701
2-(2-chloroacetamido)-3,4-hydroxythiophene	-3.659

p-tolylphosphonicacid	-3.653
1-(3,5-hydroxyphenyl)-1H-pyrrole-3-hydroxy-2,5-dione	-3.607
5,6-dihydroxy-2-benzofuran-1(3H)-one	-3.588
1-(2-furyl)-2-(1H-1,2,4-triazol-1-yl)-2-propen-1-one	-3.582
1-(3,5-hydroxyphenyl)-1H-pyrrole-3,4-dichloro-2,5-dione	-3.579
[4-(4-chlorophenyl)-4,5-dihydro-1H-pyrazol-3-yl](2-furyl)methanone	-3.493
3-hydroxylbutyricacid-2-furanamine	-3.447
Clobazam	-3.441
N3-(cyclopropylmethyl)-N-(3,5-dimethoxyphenyl)-N3-propyl-b-alaninamide	-3.368
[4-(4-chlorophenyl)-4,5-dihydro-1H-pyrazol-3-yl](2-furyl)methanone	-3.349
1-(3,5-hydroxyphenyl)-1H-pyrrole-3-chloro-2,5-dione	-3.313
carbazole	-3.268
1-(3,5-hydroxyphenyl)-1H-pyrrole-2,5-dione	-3.235
2-(2-chloroacetamido)-3,4-hydroxythiophene	-3.216
phenyl(propyl)(carbamoyl)phosphine	-3.190
N-2,6-trichloroquinoneimine	-3.164
2-(2-chloroacetamido)-3,4-hydroxythiophene	-3.110
1-(3,5-hydroxyphenyl)-1H-pyrrole-3-methyl-2,5-dione	-3.078
3,5-dihydroxybenzamide	-3.009
4-hydroxyl-2-butenoicacid	-2.965
pirfenoxone	-2.947
phenyl(dipropyl)phosphine	-2.824
tetrahydroxy-1,4-benzoquinone	-2.761
furo[3,4-b]pyrazine-2,3(1H,4H)-dione	-2.701
4-chloro-3,5-dihydroxybenzoic acid	-2.677
phenyl(propyl)(hydroxyethyl)phosphine	-2.597

furo[3,4-b]pyrazine-2,3(1H,4H)-dione	-2.536
N-propyl gallate	-2.399
1,2-di(2-furyl)-2-(hydroxyimino)ethanone	-2.377
5-(2-furyl)-5-methyl-2,4-imidazolidinedione	-2.125
3-(2-chloroacetamido)-5-hydroxythiophene	-1.524
chlorzoxazone	-1.489
5-(2-furyl)-5-methyl-2,4-imidazolidinedione	-1.474
2-furanamine-3-phenylpropanoiacid	Failed
capsidiol	Failed
2,5-diamino-3,6-dichloro-1,4-benzoquinone	Failed
methyl 3-(2,5-dioxo-2,5-dihydro-1H-pyrrol-1-yl)-1-benzofuran-2-carboxylate	Failed

References

(1) Read, J.; Winter, V.; Eszes, C.; Sessions, R.; Brady, R. Structural Basis for Altered Activity of M- and H-isozyme Forms of Human Lactate Dehydrogenase. *Proteins: Struct., Funct., Genet.* **2001**, *43*, 175–185.

(2) Schrödinger Release, LigPrep, version 3.6, Schrödinger, LLC, New York, NY. 2015.

(3) Friesner, R. A.; Murphy, R. B.; Repasky, M. P.; Frye, L. L.; Greenwood, J. R.; Halgren, T. A.; Sanschagrin, P. C.; Mainz, D. T. Extra Precision Glide: Docking and Scoring Incoporating a Model of Hydrophobic Enclosure for Protein-Ligand Complexes. *Journal of Medicinal Chemistry* **2006**, *49*, 6177–6196.

(4) Friesner, R. A.; Banks, J. L.; Murphy, R. B.; Halgren, T. A.; Klicic, J. J.; Mainz, D. T.; Repasky, M. P.; Knoll, E. H.; Shaw, D. E.; Shelley, M. et al. Glide: A New Approach for Rapid, Accurate Docking and Scoring. 1. Method and Assessment of Docking Accuracy. *Journal of Medicinal Chemistry* **2004**, *47*, 1739–1749.

(5) Halgren, T. A.; Murphy, R. B.; Friesner, R. A.; Beard, H. S.; Frye, L. L.; Pollard, W. T.; Banks, J. L. Glide: A New Approach for Rapid, Accurate Docking and Scoring. 2. Enrichment Factors in Database Screening. *Journal of Medicinal Chemistry* **2004**, *47*, 1750–1759.

(6) Small-Molecule Drug Discovery Suite, Glide, version 6.9, Schrödinger, LLC, New York, NY. 2015.

(7) Brooks, B.; Bruccoleri, R.; Olafson, B.; States, D.; Swaminathan, S.; Karplus, M. CHARMM: A Program for Macromolecular Energy, Minimization, and Dynamics Calculations. *J. Comput. Chem.* **1983**, *4*, 187–217.

(8) Brooks, B. R.; Brooks, C. L.; Mackerell, A. D.; Nilsson, L.; Petrella, R. J.; Roux, B.; Won, Y.; Archontis, G.; Bartels, C.; Boresch, S. et al. CHARMM: The Biomolecular Simulation Program. *J. Comp. Chem.* **2009**, *30*, 1545–1614.

(9) Gao, J.; Amara, P.; Alhambra, C.; Field, M. A Generalized Hybrid Orbital (GHO) Approach for the Treatment of Link-Atoms Using Combined QM/MM Potentials. *J. Phys. Chem. A* **1998**, *102*, 4714–4721.

(10) Dewar, M.; Zoebisch, E.; Healy, E.; Stewart, J. Development and Use of Quantum Mechanical Molecular Models. AM1: A New General Purpose Quantum Mechanical Molecular Model. *J. Am. Chem. Soc.* **1985**, *107*, 3902–3909.

(11) Field, M.; Bash, P.; Karplus, M. A Combined Quantum Mechanical and Molecular Mechanical Potential for Molecular Dynamics Simulations. *J. Comput. Chem.* **1990**, *11*, 700–733.

(12) Quaytman, S.; Schwartz, S. Reaction Coordinates of an Enzymatic Reaction Revealed by Transition Path Sampling. *Proc. Natl. Acad. Sci. USA* **2007**, *104*, 12253–12258.

(13) Basner, J. E.; Schwartz, S. D. How Enzyme Dynamics Helps Catalyze a Reaction, in Atomic Detail: A Transition Path Sampling Study. *J. Am. Chem. Soc.* **2005**, *127*, 13822–13831.

(14) Quaytman, S.; Schwartz, S. Comparison Studies of the Human Heart and Bacillus stearothermophilus LDH by Transition Path Sampling. *J. Phys. Chem. A* **2009**, *113*, 1892–1897.

(15) Masterson, J. E.; Schwartz, S. D. Changes in Protein Architecture and Subpicosecond Protein Dynamics Impact the Reaction Catalyzed by Lactate Eehydrogenase. *J. Phys. Chem. A* **2013**, *117*, 7107–7113.

(16) Vanommeslaeghe, K.; Hatcher, E.; Acharya, C.; Kundu, S.; Zhong, S.; Shim, J.; Daria, E.; Guvench, O.; Lopes, P.; Vorobyov, I. et al. CHARMM General Force Field: A Force Field for Drug-Like Molecules Compatible with the CHARMM All-Atom Additive Biological Force fields. *J. Comput. Chem.* **2010**, *31*, 671–690.

(17) Vanommeslaeghe, K.; MacKerell Jr., A. D. Automation of the CHARMM General Force Field (CGenFF) I: Bond Perception and Atom Typing. *J. Chem. Inf. Model.* **2012**, *52*, 3144–3154.

(18) Vanommeslaeghe, K.; Raman, E. P.; MacKerell Jr., A. D. Automation of the CHARMM General Gorce Gield (CGenFF) II: Assignment of Bonded Parameters and Partial Atomic Charges. *J. Chem. Inf. Model.* **2012**, *52*, 3155–3168.

(19) Jorgensen, W.; Chandrasekhar, J.; Madura, J.; Impey, R.; Klein, M. Comparison of Simple Potential Functions for Simulating Liquid Water. *J. Chem. Phys.* **1983**, *79*, 926–935.